A Non-Contact Interconnection Through an Electrically Thick Ground Plate Common to Two Microstrip Lines

Marat Davidovitz, *Member, IEEE*, Robert A. Sainati, *Member, IEEE*, and Steven J. Fraasch

Abstract—**Coupling between two microstrip lines through a rectangular slot in a common, electrically thick ground plate is analyzed. The results are applied to examine the properties of a vertical, noncontact line-to-line transition. An efficient and accurate design model is constructed. The model allows insight into the coupling characteristics of the device with minimal computational effort. Measured results are used to verify the efficacy of the solution. Analytical or highly convergent forms of the model parameters are derived whenever possible.**

I. Introduction

In certain applications a vertical interconnection between circuit layers or modules separated by a thick ground plate is required. A thick plate may act as a heat-sink or as a housing for modules requiring cavity isolation. Soldered probe vias may present manufacturing reliability problems. An alternative, non-contact transition is desirable in such instances. A model for coupling between two microstrip lines through a thick ground is presented in this paper. Numerical efficiency and insight into the coupling mechanisms are emphasized in the construction of the model.

A number of transmission line interconnections of the type considered here have been analyzed [1], [2], [5], [9]. In the cited studies the separating walls were taken to be thin relative to the wavelength. The aim of the investigation reported here is to demonstrate feasibility of low-loss vertical interconnection through electrically-thick ground plates, and to provide an efficient solution suitable for first-pass designs, trade-off studies and inclusion in CAD procedures.

The derivation of the model is outlined in Section I. The assumptions are presented and discussed. Even-odd mode decomposition is applied to reduce the scope of the electromagnetic problem. Mathematical procedures used to obtain the solution are described.

In Section II the numerical properties of the solution are discussed. Computational benchmarks are given for a prototypical example. A comparison of measured data with the results calculated using the model is presented.

Manuscript received April 16, 1994; revised August 8, 1994.

M. Davidovitz is with Rome Laboratory, Hanscom AFB, MA 01731–3010 USA.

R. Sainati is with CSIRO, Australia.

S. J. Fraasch is with Alliant Techsystems, Hopkins, MN USA.

IEEE Log Number 9408558.

II. Formulation

A four-port coupler is constructed by placing two identical microstrip lines on the opposite sides of a ground plate, perforated by a rectangular slot. The microstrip conductors are assumed to be parallel to one another, their center lines bisecting the long dimension of the slot. Moreover, they are taken to be perfect conductors of infinitesimal thickness.

The coupling region in the aforementioned geometry is depicted in Fig. 1. The aperture, dimensioned $a \times b$; $a > b$ may be filled, e.g. a dielectric plug (ϵ_p) may be used to create a hermetic seal, enhance the coupling, and/or decrease the required aperture dimensions. To simulate possible imperfections (air gaps) in the fabrication process, a small region of thickness t_m, close to the aperture opening, is assigned a different dielectric constant (ϵ_m).

The structure possesses a number of symmetries, most notably mirror symmetries with respect to the x-y and y-z planes. The former can be exploited to effect an even-odd mode decomposition, with a concomitant reduction of the boundary value problem for the four-port coupler to two simpler auxiliary two-port problems. The latter involve the portion of the original structure located on one side of the x-y symmetry plane. The symmetry plane is backed by Perfect Magnetic or Electric Conductor (PMC or PEC), depending on whether the even- or odd-mode case is considered.

As a consequence of the symmetries, the 4×4 scattering matrix descriptor of the coupler contains at most four unique elements. Moreover, the even-odd mode approach permits the expression of the non-redundant elements in terms of the reflection and transmission coefficients characterizing the two auxiliary solutions [8].

Either of the two-port structures obtained as a result of the even-odd decomposition belong to a wide class of transmission line-to-slot coupling problems. Most thoroughly studied are those involving slots in hollow rectangular waveguides [3]. The approach taken in these classic studies is not directly applicable to the problem at hand due to the lack of simple expressions for the microstrip line Green function. Therefore, some assumptions will be made in order to facilitate an analysis of the coupler. Specifically, it will be assumed that

- $b \ll \lambda_g$; where $\lambda_g = \frac{2\pi}{\beta_g} \equiv$ quasi-TEM transmission line wavelength. This condition will be used as a justification for retaining only the quasi-TEM mode currents to ac-

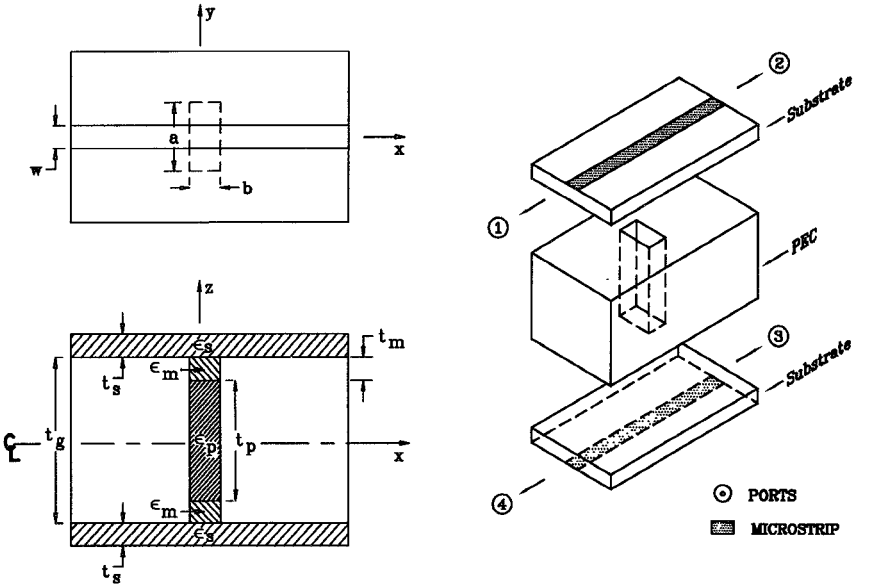

Fig. 1. Description of the coupling region.

count for the boundary conditions on the strip. To put it somewhat differently, the presence of the aperture will not alter the quasi-TEM nature of the transmission line field—rather it will affect its amplitude only.

- To obtain a computationally efficient solution, it is assumed that the aperture fields are adequately represented by the fundamental TE_{10} mode associated with the aperture cross-section.

Under the prescribed constraints, analyses performed in [4], [5] show that the aperture represents a series load on the transmission line, with the equivalent admittance approximately given by the following formula:

$$Y \approx -\frac{\int_{S_a}\int_{S_a} \mathbf{M}_a \cdot \bar{\mathbf{G}} \cdot \mathbf{M}_a \, ds\, ds'}{\left[\int_{S_a} \mathbf{M}_a \cdot \mathbf{H}_m \cos\beta_g x \, ds\right]^2} \tag{1}$$

where

$$\mathbf{M}_a(x,y) = \mathbf{E}_a(x,y) \times \hat{\mathbf{z}} = \hat{\mathbf{y}}\sqrt{\frac{2}{ab}}\cos\frac{\pi}{a}y = -\hat{\mathbf{h}}_{10}(x,y)$$

$\mathbf{H}_m(y,z), \beta_g \equiv$ quasi-TEM_x microstrip-mode transverse field and propagation constant

$S_a \equiv$ aperture area.

Assuming a coordinate system in which the aperture is located at $z = 0$ (x-y plane), the Green function dyad $\bar{\mathbf{G}}$ can be expressed as follows:

$$\bar{\mathbf{G}}(\mathbf{R},\mathbf{R}') = \bar{\mathbf{G}}_+(\mathbf{r},\mathbf{r}';z=0,z'=0) + \bar{\mathbf{G}}_-(\mathbf{r},\mathbf{r}';z=0,z'=0) \tag{2}$$

where

$\bar{\mathbf{G}}_+ \equiv$ Green function for a PEC-backed dielectric slab

$\bar{\mathbf{G}}_- \equiv$ Green function for a waveguide cavity, terminated in either PEC or PMC

$\mathbf{R} = x\hat{\mathbf{x}} + y\hat{\mathbf{y}} + z\hat{\mathbf{z}}$; $\mathbf{r} = x\hat{\mathbf{x}} + y\hat{\mathbf{y}}$.

The '$\approx$' sign in (1) is used to emphasize the fact that the assumptions made in its derivation render this relationship approximate even if the exact aperture distribution $\mathbf{M}_a$ is known.

A. Evaluation of Y

For purposes of evaluation, the right hand side of formula (1) can be broken up into three distinct terms.

A closed form result is obtained for the term to be denoted Y_{a_-}. Since the Green function $\bar{\mathbf{G}}_-$ is written in terms of the orthonormal waveguide modes associated with slot cross-section [10], a straightforward calculation yields

$$Y_{a_-} \equiv -\int_{S_a}\int_{S_a} \mathbf{M}_a \cdot \bar{\mathbf{G}}_- \cdot \mathbf{M}_a \, ds\, ds' = Y'_{10} \tag{3}$$

where Y'_{10} is the input admittance of the TE_{10}-mode equivalent transmission line circuit representing the slot waveguide. This quantity is given by the following formulas

$$Y'_{10} = Y_{cm}\frac{\vec{Y}(t_m) + Y_{cm}\coth k_{zm}t_m}{Y_{cm} + \vec{Y}(t_m)\coth k_{zm}t_m} \tag{4}$$

$$\vec{Y}(t_m) = \begin{cases} Y_{cp}\coth\frac{k_{zp}t_p}{2} & \text{PEC} \\ Y_{cp}\tanh\frac{k_{zp}t_p}{2} & \text{PMC} \end{cases} \tag{5}$$

with $Y_{c\alpha} = \frac{\omega\epsilon_0\epsilon_{r\alpha}}{-j\,k_{z\alpha}}$; $k_{z\alpha} = \sqrt{(\frac{\pi}{a})^2 - k_0^2\epsilon_{r\alpha}}$; $k_0 = \omega\sqrt{\mu_0\epsilon_0}$, and $\alpha = m, p$

The equivalent aperture admittance in the ground-backed slab environment is designated Y_{a_+} and is defined as follows

$$Y_{a_+} \equiv -\int_{S_a}\int_{S_a} \mathbf{M}_a \cdot \bar{\mathbf{G}}_+ \cdot \mathbf{M}_a \, ds\, ds'. \tag{6}$$

The Green function $\bar{\mathbf{G}}_+$ can be written in the following form

$$\bar{\mathbf{G}}_+(\mathbf{r},\mathbf{r}';z=0,z'=0) = \frac{1}{(2\pi)^2}\iint_{-\infty}^{\infty}\tilde{\bar{\mathbf{G}}}_+(\mathbf{k}_t;z=0,z'=0)e^{-j\,\mathbf{k}_t\cdot(\mathbf{r}-\mathbf{r}')}\,d\mathbf{k}_t \tag{7}$$

where $\mathbf{k}_t = k_x\hat{\mathbf{x}} + k_y\hat{\mathbf{y}} = k_t(\hat{\mathbf{x}}\cos\alpha + \hat{\mathbf{y}}\sin\alpha)$, and

$$\tilde{\bar{\mathbf{G}}}_+(\mathbf{k}_t;z=0,z'=0) = -I'(k_t)(\hat{\mathbf{z}}\times\hat{\mathbf{k}}_t)(\hat{\mathbf{z}}\times\hat{\mathbf{k}}_t) - I''(k_t)\hat{\mathbf{k}}_t\hat{\mathbf{k}}_t \tag{8}$$

$$I(k_t) = Y_{cs}\frac{Y_{cs}+Y_{c0}\coth k_{zs}t_s}{Y_{c0}+Y_{cs}\coth k_{zs}t_s} \tag{9}$$

with $Y'_{c\alpha} = \frac{\omega\epsilon_0\epsilon_{r\alpha}}{-j\,k_{z\alpha}}$; $Y''_{c\alpha} = \frac{-j\,k_{z\alpha}}{\omega\mu_0}$; $k_{z\alpha} = \sqrt{k_t^2 - k_0^2\epsilon_{r\alpha}}$; and $\alpha = s, 0$ The difficulties encountered in the evaluation of (6) and (7) are well-known. Under certain circumstances, the expression for Y_{a_+} can be put into a more convenient and suggestive form.

Consider a situation in which the condition $a \ll \lambda_0/\sqrt{\epsilon_{rs}}$ (λ_0 is the free-space wavelength) is satisfied. Equivalently, this implies that the frequency of operation $f \ll 2f_{c10}\sqrt{\epsilon_p/\epsilon_s}$, where f_{c10} is the cutoff frequency of the aperture.[1]

Within the frequency range satisfying the stated requirement, a quasistatic evaluation of the Green function, and the aperture admittance term Y_{a_+} is adequate. As $k_0 \to 0$ the spectral functions defined in (9) can be approximated as follows:

$$I'(k_t) \approx \frac{j\,\omega\epsilon_0\epsilon_{rs}}{k_t}\,\frac{\epsilon_{rs}+\coth k_t t_s}{1+\epsilon_{rs}\coth k_t t_s} = \frac{j\,\omega\epsilon_0\epsilon_{rs}}{k_t}\sum_{n=0}^{\infty}(2-\delta_{0n})q^n e^{-2nk_t t_s} \tag{10}$$

$$I''(k_t) \approx \frac{k_t}{j\omega\mu_0} \tag{11}$$

where $q \equiv (1-\epsilon_{rs})/(1+\epsilon_{rs})$, and δ_{0n} is the Kronecker symbol.

Because of their relative simplicity, the inverse Fourier transform of these terms can be carried out explicitely. The quasistatic approximation can then be written in the following manner:

$$Y_{a_+} = G_+(\omega) + j\omega C_+ + \frac{1}{j\omega L_+} \tag{12}$$

where

$G_+(\omega)$—aperture conductance

C_+—aperture capacitance

L_+—aperture inductance.

The conductance was computed using the far-field space- and surface-wave forms of the Green function. The formulas for these circuit quantities are given in the Appendix.

When the problem lies outside the quasistatic regime, the improper integrals appearing in the Green function definition (7) must be evaluated. This evaluation can be expedited by noting that the zero-frequency approximations in (10) and (11) are also the dominant asymptotic terms of the integrand representing the Fourier transform of the Green function. Therefore, the following formula provides an efficient scheme for calculating the improper integrals:

$$Y_{a_+} = -\int_{S_a}\int_{S_a}\mathbf{M}_a\cdot\bar{\mathbf{G}}_+\cdot\mathbf{M}_a\,ds\,ds' \tag{13}$$

$$= -\frac{1}{(2\pi)^2}\int\int_{-\infty}^{\infty}\tilde{\mathbf{M}}_a\cdot\tilde{\bar{\mathbf{G}}}_+\cdot\tilde{\mathbf{M}}_a\,d\mathbf{k}_t \tag{14}$$

$$= -\frac{1}{(2\pi)^2}\int\int_{-\infty}^{\infty}\tilde{\mathbf{M}}_a\cdot[\tilde{\bar{\mathbf{G}}}_+ - \tilde{\bar{\mathbf{G}}}_+(k_0\to 0)]\cdot\tilde{\mathbf{M}}_a d\mathbf{k}_t + j\omega C_+ + \frac{1}{j\omega L_+}. \tag{15}$$

The tilde marks the Fourier transform of a function and $\tilde{\bar{\mathbf{G}}}_+(k_0 \to 0)$ represents the asymptotic form of $\tilde{\bar{\mathbf{G}}}_+$ obtained by substituting (10) and (11) into (8).

The denominator in (1) represents the square of the projection of the quasi-TEM mode field onto the aperture distribution. The inverse of this projection integral will be denoted by n, i.e.

$$n^{-1} = \int_{S_a}\mathbf{M}_a\cdot\mathbf{H}_m\cos\beta_g x\,ds. \tag{16}$$

The expression for the tangential magnetic field at the ground plane of a microstrip line is required to calculate this quantity. A good first-order expression for the field can be obtained using statics and a reasonable current approximation. Assuming a strip current density

$$J_x(y) = \frac{2}{\pi w}\,\frac{1}{\sqrt{1-(\frac{2y}{w})^2}}\quad;\qquad |y|\le w/2 \tag{17}$$

and using free-space static Green function yields

$$H_{my}(y,z=0) = \frac{t_s}{\pi\sqrt{\xi+2\sqrt{\zeta\nu}}}\left(\frac{1}{\sqrt{\zeta}}+\frac{1}{\sqrt{\nu}}\right) \tag{18}$$

where

$$\zeta = t_s^2 + \left(y+\frac{w}{2}\right)^2 \tag{19}$$

$$\xi = 2\left[t_s^2 + y^2 + \left(\frac{w}{2}\right)^2\right] \tag{20}$$

$$\nu = t_s^2 + \left(y-\frac{w}{2}\right)^2. \tag{21}$$

The free-space Green function was used because in the static limit the magnetic field is not affected by the dielectric slab's presence. The form of the magnetic field distribution obtained in this manner was compared with that calculated using a dynamic, grounded-slab Green function. For the range of transmission line parameters considered, the analytical expression (18) provides a very good approximation. The uniform current distribution was tried as an alternative to (17). The results were not significantly different, although the former may be more appropriate for wide lines.

The admittance Y can now be expressed as follows:

$$Y = Y_j + n^2 Y_{a_-} \tag{22}$$

[1] Because the gap (t_m) is small, the cutoff frequency of the aperture is primarily determined by the dielectric constant ϵ_p.

TABLE I
COUPLER PARAMETERS FOR FIGS. 3–5

Figure #	a	b	w	t_s	t_m	ϵ_{rs}	ϵ_{rp}	$t_g (= t_p)$	OC Stubs [2)]
3	500	100	196	62	≈ 0	2.2	10.5±0.25	50	650
4	500	100	196	62	≈ 0	2.2	10.5±0.25	300	650
5	500	100	196	62	≈ 0	2.2	10.5±0.25	1000	650

Notes:
1) All dimensions are in mils
2) Measured with respect to the aperture center

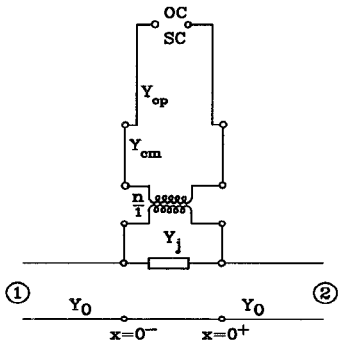

Fig. 2. Equivalent circuit of the slot in the microstrip line.

where in general

$$Y_j = n^2 Y_{a_+} = n^2 \left[G_+(\omega) + j\omega C_+(\omega) + \frac{1}{j\omega L_+(\omega)} \right]$$

– junction admittance

$Y_{a_-} = Y'_{10}$ – TE_{10} modal admittance for a short- or open-circuited guide

n – transformer turn ratio

When the aperture dimension are such that $a \ll \lambda_0/\sqrt{\epsilon_{rs}}$, static capacitance C_+ and inductance L_+ values can be used. An interpretation of (22) in the form of an equivalent circuit [3] is displayed in Fig. 2.

The model can be extended, under the same constraints, to couplers containing nonidentical transmission lines. The equivalents circuit for such couplers would include two different junction admittances $Y_{j1,2}$ and transformers with turn ratios $n_{1,2}$, interconnected by a transmission line representing the slot waveguide.

III. NUMERICAL RESULTS AND EXPERIMENTAL VALIDATION

A. Numerical Properties of the Solution

A computer implementation of the proposed solution was used to determine its computational characteristics. By far the most demanding is the calculation of the aperture admittance Y_{a_+}. If the analytical regime satisfies the quasistatic condition $a \ll \lambda_0/\sqrt{\epsilon_{rs}}$, the effort is reduced manyfold. In that instance the aperture capacitance and inductance are frequency-independent and need not be recalculated during a frequency scan. It has been found that the quasistatic formulas are accurate well beyond the range allowed by the constraining condition. In quantitative terms, excellent approximation to the susceptance is obtained when $a\sqrt{\epsilon_{rs}}/\lambda_0 < 0.2$, and good agreement is still observed if $a\sqrt{\epsilon_{rs}}/\lambda_0 < 0.75$. The fact that the aperture field is not uniform, but rather is concentrated around its center, thus making the "effective field volume" smaller than the physical volume, may offer an explanation for the efficacy of the approximate formulas over a wider-than-expected range. The integrals representing the aperture conductance have benign integrands and can be evaluated using low-number Gaussian quadrature. A frequency scan comprising 100 points can then be carried out in a fraction of a second on any work-station.

When the problem lies outside the quasistatic range, the aforementioned calculation of Y_{a_+} must be augmented by the addition of higher-order, frequency-dependent capacitance and inductance terms. Those are obtained by evaluating the imaginary part of the spectral integral in (15). The integrand therein rapidly decays for large values, permitting reduction of the integration range radius to $20k_0$. Using an adaptive two-dimensional quadrature procedure in the IMSL [7] library data can be obtained at a rate of approximately four seconds per frequency point on a Sun (SPARC 10) workstation. Code optimization, particularly elimination of the overhead associated with the adaptive quadrature algorithm, can be expected to reduce this time significantly.

B. Experimental Validation

To test the effectiveness of the proposed solution an experiment was carried out with a noncontact microstrip-to-microstrip transition. Ports designated 2 and 4 in Fig. 1 were terminated with open-circuit stubs (the open-ends of the stubs were simulated using excess-capacitance formulas). The parameters of the resulting two-port device are summarized in Table I. A series of Return Loss (RL) and Insertion Loss (IL) versus frequency plots for the interconnection are presented in Figs. 3–5. The thickness of the ground plate ranges from $t_g = 50$ mils to $t_g = 1000$ mils. The frequency range[2] is 2–6 GHz and the aperture (filled with Rogers 6010.5 dielectric $\epsilon_{rp} = 10.5 \pm 0.25$) has a cutoff frequency of 3.64 GHz. The thickness t_m was set to zero in calculation. It should be noted, however, that the data, particularly the resonant frequencies, were found to be very sensitive to small variations in this parameter, possibly due to the high dielectric constant of the plug. Therefore, even a small air-gap (t_m), unintentionally

[2]The experimental data is unreliable close to 6 GHz due to resonances in the TRL calibration standards.

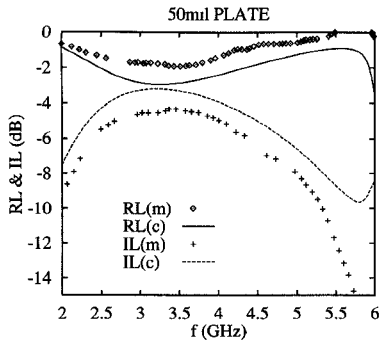

Fig. 3. Measured (m) and calculated (c) return and insertion loss for a two-port coupler with a 50-mil ground plate (for dimensions refer to Table I).

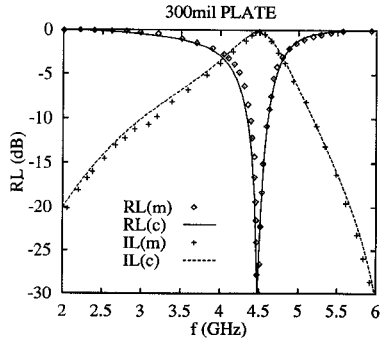

Fig. 4. Measured (m) and calculated (c) return and insertion loss for a two-port coupler with a 300-mil ground plate (for dimensions refer to Table I).

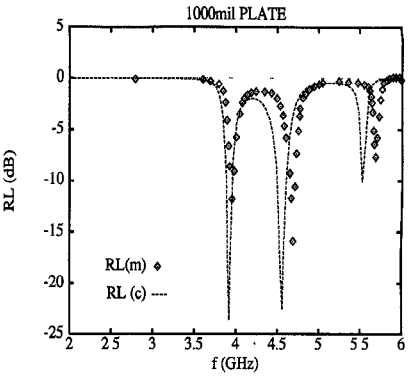

(a)

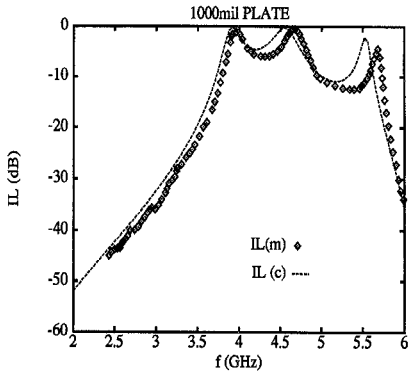

(b)

Fig. 5. Measured (m) and calculated (c) return and insertion loss for a two-port coupler with a 1000-mil ground plate (for dimensions refer to Table I).

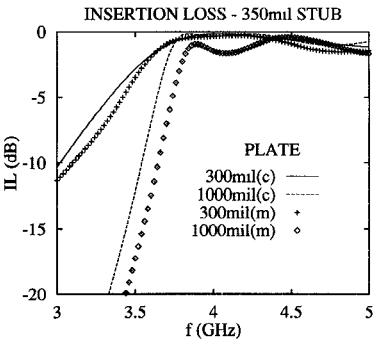

Fig. 6. Measured(m) and calculated(c) return and insertion loss for the couplers in Figs. 4 and 5 with the stubs shortened to 350 mils (for dimensions refer to Table I).

introduced in the fabrication process, can be a source for some of the observed discrepancies between the computed and measured results. The results were calculated using the quasistatic approximation.

For the chosen open-circuit stubs' length, the transmission line current (and consequently the magnetic field) at the aperture location is large over a fairly wide frequency range, centered around 3.1 GHz—the frequency at which the stub is a quarter of the guided wave length. The resulting coupling is too tight and critical coupling required for complete transmission is achieved only when the frequency is close to the resonant frequency of the open-ended waveguide resonator formed by the slot in the ground-plate. This may provide a qualitative explanation for the multiply-resonant response observed for thicker ground plates. The measured and computed data agree well, particularly in characterizing the frequency behavior of the first resonance.

Reduction of the stubs' length loosens the line-aperture coupling and allows for low-insertion-loss transmission over a wide band above the cutoff frequency of the aperture. The insertion loss response of the coupler characterized in Table I, with stub lengths reduced to 350 mils, is depicted in Fig. 6.

IV. Conclusion

An efficient first-order model describing coupling through a slot aperture in a thick ground plate common to two microstrip lines was constructed. The model tracks experimental data well. The feasibility of a low-loss, non-contact via in an electrically-thick ground plate was demonstrated.

Appendix

Let

$$\tau_n \equiv \frac{2nt_s}{a};\ \beta \equiv \frac{b}{a};\ q \equiv \frac{(1-\epsilon_{rs})}{(1+\epsilon_{rs})}. \tag{23}$$

A. Aperture Capacitance

$$C_+ = \frac{\epsilon_0 \epsilon_{rs} a^2}{\pi b} \sum_{n=0}^{\infty} (2-\delta_{0n})\, q^n P(\tau_n, \beta) \tag{24}$$

$$P(\tau_n, \beta) = \int_0^1 g(u)\, F(u, \tau_n, \beta)\, du \tag{25}$$

$$F(u,\tau_n,\beta) = 2\sqrt{\beta^2+\tau_n^2+u^2} - 2\sqrt{\tau_n^2+u^2} + 2\tau_n \log\left[\frac{\tau_n+\sqrt{\tau_n^2+u^2}}{\tau_n+\sqrt{\beta^2+\tau_n^2+u^2}}\right] \quad (26)$$

$$g(u) = (1-u)\cos\pi u + \frac{1}{\pi}\sin\pi u. \quad (27)$$

For $0.05 \le \beta \le 1$ the integral in (25) can be evaluated to at least 3 significant digits using a 10-point Gaussian rule. Moreover, when $\tau_n > 3$ it can be replaced with the asymptotic result

$$P(\tau_n,\beta) = \frac{2}{\pi^2}[F(1,\tau_n,\beta)+F(0,\tau_n,\beta)] + \Delta\ ;\ 0<\beta\le 1 \quad (28)$$

with $\Delta < 2\times 5^{-4}$ and relative error of at most 1%.

B. Aperture Inductance

$$L_+ = \frac{2\pi}{\mu_0 b}Q(\beta) \quad (29)$$

$$Q(\beta) = -\frac{1}{\pi^2} - \beta\left[\frac{2-\pi \mathrm{Si}(\pi)}{\pi^2}\right] - \int_0^1 i(u)\,H(u,\beta)\,du \quad (30)$$

$$H(u,\beta) = \sqrt{\beta^2+u^2} - \beta\log(\beta+\sqrt{\beta^2+u^2}) \quad (31)$$

$$i(u) = (1-u)\cos\pi u - \frac{1}{\pi}\sin\pi u \quad (32)$$

where β is defined in (23) and $\mathrm{Si}(\cdot)$ is the sine integral. Coordinate transformations described in [6] were used in the derivation of the capacitance and inductance formulas.

C. Aperture Conductance

Space- and surface-wave radiation contribute to power dissipation in the equivalent aperture conductance. Therefore it is appropriate to write $G_+(\omega) = G_{\mathrm{rad}}(\omega) + G_{\mathrm{sw}}(\omega)$.

Space-wave conductance:

$$G_{\mathrm{rad}} = \int_0^{\pi/2} d\phi \int_0^{\pi/2} d\theta\ E(\theta,\phi) \quad (33)$$

$$E(\theta,\phi) = \frac{k_0^4}{\pi^2\eta_0}\cos^2\theta\sin\theta\tilde{M}_a^2(k_x,k_y) \times \left[R_1(\theta)\cos^2\phi + R_2(\theta)\sin^2\phi\right] \quad (34)$$

$$R_1(\theta) = \frac{\epsilon_{rs}^2}{k_{z0}^2\epsilon_{rs}^2\cos^2 k_{zs}t_s + k_{zs}^2\sin^2 k_{zs}t_s} \quad (35)$$

$$R_1(\theta) = \frac{(k_{zs}/k_0)^2}{k_{zs}^2\cos^2 k_{zs}t_s + k_{z0}^2\sin^2 k_{zs}t_s} \quad (36)$$

$$\tilde{M}_a(k_x,k_y) = \sqrt{\frac{8\pi^2 b}{a^3}}\ \frac{\sin(k_x b/2)}{(k_x b/2)}\ \frac{\cos(k_y a/2)}{(\pi/a)^2-k_y^2} \quad (37)$$

where

$$k_{z0} = k_0\cos\theta;\ k_{zs} = k_0\sqrt{\epsilon_{rs}-\sin^2\theta};\quad k_x = k_0\sin\theta\cos\phi;\ k_y = k_0\sin\theta\sin\phi \quad (38)$$

Surface-wave conductance:

$$G_{\mathrm{sw}} = \frac{1}{D(\beta_0,\beta_s)}\int_0^{\pi/2} d\phi\ \tilde{M}_a^2(k_{xc},k_{yc})\cos^2\phi \quad (39)$$

$$D(\beta_0,\beta_s) = \frac{\pi\eta_0}{k_0\epsilon_{rs}}\cos(\beta_s t_s)\sin(\beta_s t_s) \times \left[\frac{k_0^2(\epsilon_{rs}-1)}{\beta_0^2\beta_s} + \frac{t_s(\beta_s^2+\beta_0^2\epsilon_{rs}^2)}{\beta_0\beta_s\epsilon_{rs}}\right] \quad (40)$$

where β_0, β_s satisfy the dispersion relation

$$\beta_s = \beta_0\epsilon_{rs}\cot\beta_s t_s \qquad \beta_s^2+\beta_0^2 = k_0^2(\epsilon_{rs}-1) \quad (41)$$

and

$$\beta_0 = \sqrt{k_c^2-k_0^2}\ ;\ \beta_s = \sqrt{k_0^2\epsilon_{rs}-k_c^2} \qquad k_{xc} = k_c\cos\phi;\ k_{yc} = k_c\sin\phi. \quad (42)$$

For many situations of practical interest, an approximate root of (41), which may also be used as a starting value for a numerical root search, is given by

$$(\beta_s t_s)^2 \approx \frac{1}{2}\left[\sqrt{\epsilon_{rs}^4 + 4(k_0 t_s\epsilon_{rs})^2(\epsilon_{rs}-1)} - \epsilon_{rs}^2\right]. \quad (43)$$

References

[1] M. Kumar and B. N. Das, "Coupled transmission lines," *IEEE Trans. Microwave Theory Tech.*, vol. MTT-25, no. 1, Jan. 1977.

[2] K. C. Gupta, R. Garg, and I. J. Bahl, *Microstrip Lines and Slotlines.* Norwood, MA: Artech House, 1979.

[3] A. A. Oliner, "The impedance properties of narrow radiating slots in the broad face of a rectangular waveguide—Parts I, II," *IRE Trans. Antenn. Propagat.*, vol. AP-5, no. 1, pp. 4–20, Jan. 1957.

[4] K. Nakaoka, K. Itoh, and T. Matsumoto, "Input characteristics of slot antenna for printed array antennas," *Electron. Commun. in Japan*, vol. 60-B, no. 5, pp. 77–85, 1977.

[5] N. Herscovici and D. M. Pozar, "Full-wave analysis of aperture-coupled microstrip lines," *IEEE Trans. Microwave Theory Tech.*, vol. MTT-39, no. 7, pp. 1108–1114, July 1991.

[6] L. Lewin, *Advanced Theory of Waveguides.* London: Iliffe and Sons, Ltd., 1951.

[7] *IMSL Mathematics Fortran Library, version 10.0 User's Manual.*

[8] J. Helszajn, *Passive and Active Microwave Circuits.* New York: Wiley, 1974, p. 47.

[9] A. M. Tran and T. Itoh, "Analysis of microstrip lines coupled through an arbitrarily shaped aperture in a thick ground plane," in *Proc. IEEE-MTT Symp.*, 1993, pp. 819–822.

[10] L. B. Felsen and N. Marcuvitz, *Radiation and Scattering of Waves.* Englewood Cliffs, NJ: Prentice-Hall, 1973.

Marat Davidovitz (S'81–M'81–S'82–M'82–S'82–M'86–S'86–M'87), received the B.S. (Highest Honors) and M.S. degrees in Electrical Engineering from the University of Illinois, Chicago, in 1981 and 1983, respectively, and the Ph.D. degree in Electrical Engineering from the University of Illinois, Urbana-Champaign, IL, in 1987.

From 1987 to 1988 he was an Alexander von Humboldt post-doctoral fellow at DLR, Oberpfaffenhofen, Germany. Between 1988 and 1993 he taught at the Department of Electrical Engineering, University of Minnesota, Minneapolis, MN. Since 1994 he has been with the Air Force's Rome Laboratory, Hanscom AFB, MA. Among his interests are microwave circuits and antennas, electromagnetic scattering, and woodworking.

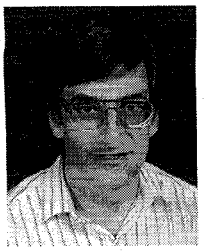

Robert A. Sainati (S'65–M'68), received the B.S.E.E. and M.S.E.E. degrees from the University of Illinois, Urbana-Champaign, IL and the Ph.D. degree in Electrical Engineering from the University of Connecticut.

He is currently at the division of Radiophysics, CSIRO Australia developing printed circuit antennas for millimeter wave wireless LAN's. Prior to joining CSIRO, he was employed by Alliant Techsystems, Hopkins, MN, where he designed millimeter wave antennas for various military systems. His first position was at the Naval Undersea Warfare Center, New London, CT developing antennas for submarine applications.

Steven J. Fraasch (M'94) received the B.S. degree from the U.S. Military Academy, West Point, NY in 1983, and the M.S. degree in Electrical Engineering from the University of Minnesota, Minneapolis, MN in 1994.

From 1983 to 1988, he served as an armor officer while on active duty with the U.S. Army. Since 1988 he has been employed by Alliant Techsystems as a principal development engineer, designing munition sensor systems. His main interest is in the area of millimeter wave microstrip antenna analysis and design.